Investigating Optical Cavities in FINESSE

Contents

1. Purpose and scope

These notes are intended as complementary study material to support and facilitate the understanding of the project. They do not replace the original FINESSE documentation or primary references, but are meant to guide the reader through the structure, assumptions, and methodology used in the accompanying notebooks. Throughout this work, we will follow conventions summarised in Ref. [1].

2. Introduction

Gravitational wave detectors are the most precise instruments for measuring length changes. Their L-shaped design directly reflects the transverse nature of gravitational perturbations, which stretch space in one direction and compress it perpendicularly, both orthogonal to the direction of propagation.
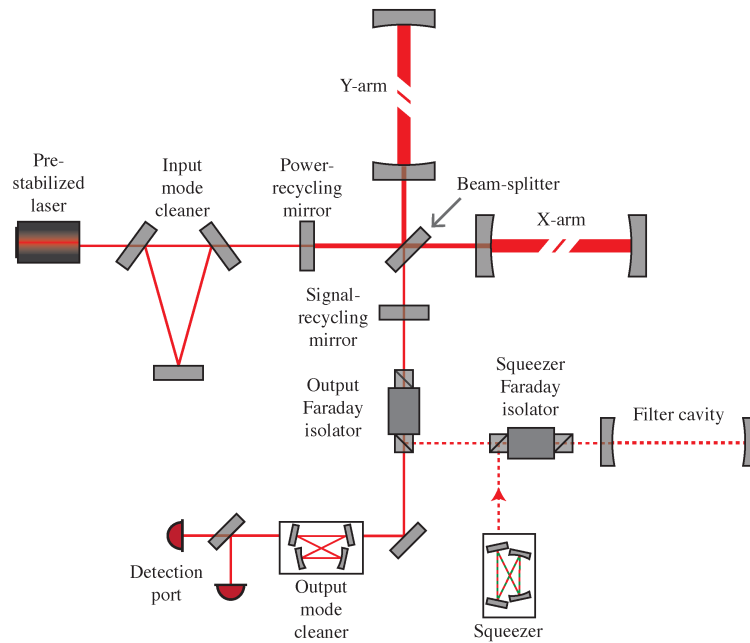
Figure 2.1: A typical 2G configuration, highlighting the additional components compared to a standard Michelson interferometer: Fabry-Perot cavities; power recycling system; input and output mode cleaning optics.

Currently, a worldwide network of second-generation (2G) interferometric detectors is operational: the two Advanced LIGO (aLIGO) observatories [2], Advanced Virgo (AdV) [3], KAGRA [4], and GEO600 [5]. While most of these evolved from first-generation (1G) designs, KAGRA was built with a 2G technology from the start. All share similar optical topologies, illustrated in Figure 2.1, which is more sophisticated than a simple Michelson interferometer and incorporates essential optical elements, each one with its own peculiarities and specific aims.

Among these complex topologies, we will focus in this workshop on optical cavities. These are the fundamental building blocks of current GW detectors, and therefore their study deserves special attention. In this short document, we aim to cover as much material as possible to help guide you toward an understanding of both FINESSE and the basic principles of optical cavities.

3.   FINESSE Basics & Cheat Sheet

In the gravitational-wave community, modeling plays an essential role in detector design and operation. GW detectors are extremely complex systems, in the sense that their operation depends on a large number of parameters. In this project, you will be introduced to modeling with FINESSE, a frequency-domain simulation tool.

In this section, we will introduce some basic modeling principles in FINESSE and present a few practical tips and tricks for working with it. In particular, we aim to answer the question: "How does one model in FINESSE?" For reference, it is helpful to keep the FINESSE documentation open while working through this section.

1. **Component library** — Since our aim is to perform optical simulations that represent real experiments, we need to model realistic optical components in FINESSE, such as mirrors, lasers, and detectors. FINESSE allows us to model almost all major optical components and detectors used in GW experiments. You can find the full list of available components and their syntax in the documentation page Model Elements. For this workshop, we will primarily build our models using mirrors, lasers, and space elements, and we will also make use of detectors to study the behavior and physics of our optical systems.

2. **Ports and nodes** — All components and elements in FINESSE use what is called a port-and-node system. These ports allow us to connect one optical component to another and define how the optics in our model are interconnected. In FINESSE, the optical system we want to simulate is represented as a network of nodes connected by optical components.

   A mirror, as shown in Fig. 3.1a, has two optical ports:

   - `p1`: the left-hand side of the mirror,
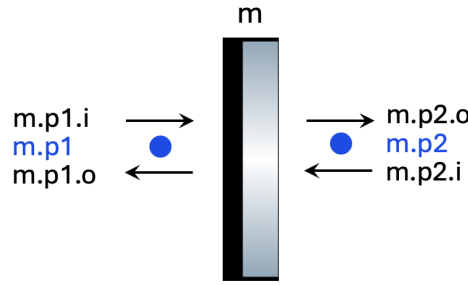   - `p2`: the right-hand side of the mirror.

   Each optical port contains two optical nodes:

   - `.i`: incoming field,
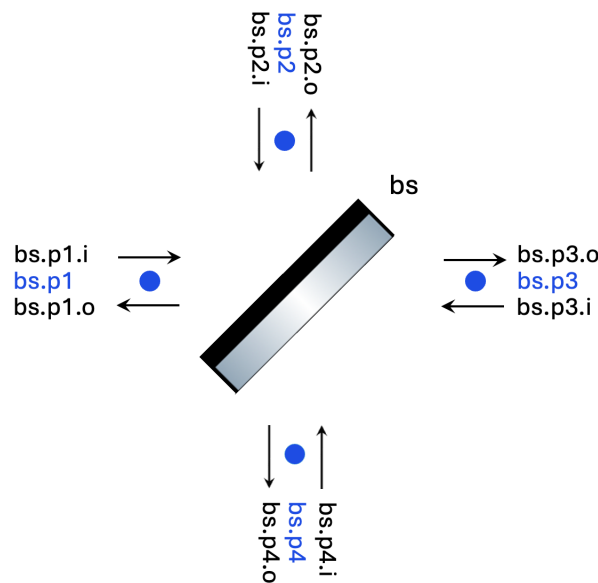   - `.o`: outgoing field.

   In total, a mirror has four optical nodes, and the arrows in the figure indicate the direction of field propagation associated with each node. Components can be connected via ports using the `space(s)` element.

   A beamsplitter requires special attention. It is described in FINESSE using the same formalism, but with four optical ports instead of two. As for mirrors, each port contains an incoming and an outgoing node, as shown in Fig. 3.1b.

3. **Beam parameter (q-parameter)** — So far, we have defined our optics and connected it using the ports and nodes system in FINESSE . Very often, we also want to specify the shape and characteristics of the Gaussian beam resonating inside our optical models. The beam is described by the so-called q-parameter (see Section 4.2.1 for more details). In FINESSE, we can define the beam in multiple ways using the `Cavity` and `Gauss` commands; see Gaussian beams. These commands will be used in the notebooks we have prepared. Whenever you want to define a fixed beam in your optical model, remember to use one of these commands.

(a) Ports and nodes for a mirror component in FINESSE.

(b) Ports and nodes for a beam splitter component in FINESSE.

Figure 3.1: Ports and nodes in Finesse.

4. **Simulation with higher-order modes (HOMs)** — To perform simulations including HOMs in FINESSE, you need to specify the maximum mode order to be included. Normally, when you define Cav or Gauss in your model, the simulation assumes only the fundamental mode (HG$_{00}$). You can enable HOMs in your simulations by defining the maxtem parameter in FINESSE, for example your_model.modes(maxtem=5). This will include all higher-order modes up to order 5 in the simulation.

5. **Actions** — Last but not least, once we have built our optical model, we usually want to change "something" and study the response of the system. This something can be, for example, the length of a space between optics, or alignment parameters (tip and tilt), and so on. This is ultimately the main goal of modeling: to vary the relevant parameters and study the corresponding physical response of the system using detectors. In our notebooks we will usually change the microscopic tuning (phi) between the optical cavities and study its characteristics (see Section 4.1.3).

To summarize, one can think of modeling in FINESSE as a three-step process, for simplicity. This is illustrated in Fig. 3.2. For the tutorial notebooks provided to you, we will usually follow
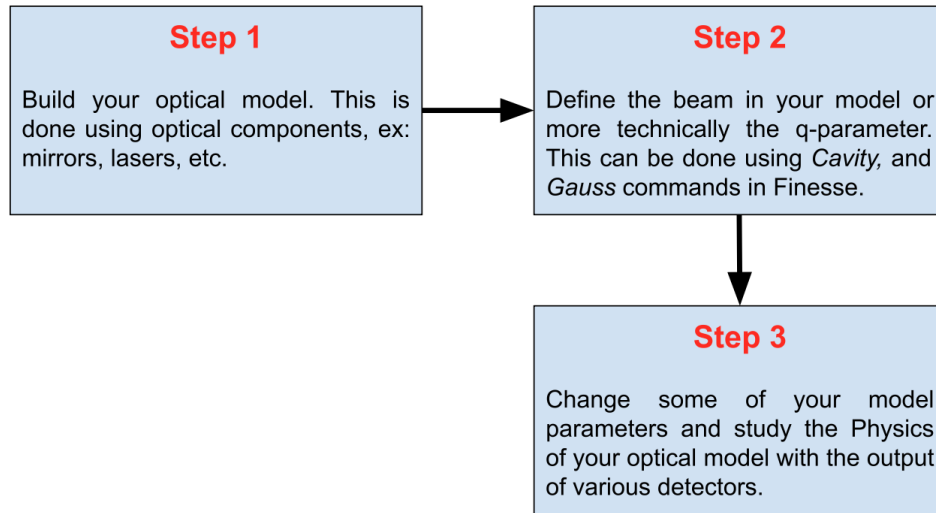
Figure 3.2: Summary of modeling in Finesse.

these steps sequentially and model optical cavities.

4. Theoretical Background

In this section, we will study the analytical description of a special class of optical cavities, namely Fabry–Perot cavities, as well as Gaussian beams.

4.1. Fabry-Perot Cavities

Fabry-Perot (FP) cavities are extensively used in GW detectors and represent the core of the optics. In the simulation tasks as part of this workshop, we will model cavities extensively and therefore it is important for us to define the important parameters and physics of these optical systems.
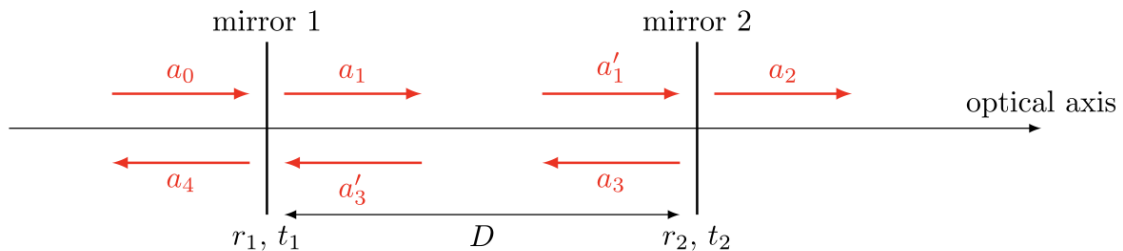
4.1.1. Field equations

Figure 4.1: Simplified schematic of a two mirror cavity. The two mirrors are defined by the amplitude coefficients for reflection and transmission. Further, the resulting cavity is characterised by its length D. Light field amplitudes are shown and identified by a variable name, where necessary to permit their mutual coupling to be computed.

Coupling relations:

$$
\begin{aligned}
a_1 &= it_1 a_0 + r_1 a_3' \\
a_1' &= e^{-ikD} a_1 \\
a_2 &= it_2 a_1' \\
a_3 &= r_2 a_1' \\
a_3' &= e^{-ikD} a_3 \\
a_4 &= r_1 a_0 + it a_3'
\end{aligned}
\tag{4.1}
$$

Based on these relations, we want to express the reflected, transmitted and circulating fields (a_4, a_2 and a_3', respectively), in terms of the input field a_0. The results are reported below:

$$
\begin{aligned}
a_4 &= a_0 \left(r_1 - \frac{r_2 t_1^2 \exp(-2ikD)}{1 - r_1 r_2 \exp(-2ikD)} \right) = a_0 \left(\frac{r_1 - r_2(t_1^2 + r_1^2)\exp(-2ikD)}{1 - r_1 r_2 \exp(-2ikD)} \right) \\
a_2 &= a_0 \frac{-t_1 t_2 \exp(-ikD)}{1 - r_1 r_2 \exp(-2ikD)} \\
a_3' &= a_0 \frac{ir_2 t_1 \exp(-2ikD)}{1 - r_1 r_2 \exp(-2ikD)}
\end{aligned}
\tag{4.2}
$$

4.1.2. Circulating field and resonance condition

Let us now assume the mirrors of the cavity are highly reflective. The situation is the following: a laser shines on mirror 1; a small fraction of the light enters the cavity, the majority is reflected. That light reflects off mirror 2, comes back to mirror 1, and keeps circulating. Meanwhile, the laser keeps injecting new light.

The key question here is: what determines whether the circulating light grows, stays constant, or decreases? The answer is interference between the light already circulating in the cavity and the newly injected light from the laser, or, in other words, the relative phase of these two waves at the point where they interfere. For clarity, let us examine two elementary interference examples.

- **Example 1: constructive interference**.

$$
E_1(t) = E_0 \cos(\omega t), \; E_2(t) = E_0 \cos(\omega t)
\tag{4.3}
$$

then

$$
E_1(t) + E_2(t) = 2E_0 \cos(\omega t)
\tag{4.4}
$$

The resulting wave has larger amplitude and intensity. This is constructive interference.

- **Example 2: destructive interference**.

Now consider two waves with the same frequency and amplitude, but out of phase by π:

$$
E_1(t) = E_0 \cos(\omega t), \; E_2(t) = E_0 \cos(\omega t + \pi)
\tag{4.5}
$$

Using the trigonometric identity

$$\cos(\theta + \pi) = -\cos\theta, \tag{4.6}$$

we have

$$E_1(t) + E_2(t) = E_0\cos(\omega t) - E_0\cos(\omega t) = 0 \tag{4.7}$$

The waves cancel each other, resulting in zero field and zero intensity. This is destructive interference.

Now let us return to the formula of the circulating power:

$$a_3' = a_0 \frac{ir_2 t_1 \exp(-2ikD)}{1 - r_1 r_2 \exp(-2ikD)} \tag{4.8}$$

We will see that maximizing the power stored inside the cavity naturally leads to a condition on the phase. Is trivial to see that the circulating power is maximum if the denominator is minimum, which translates into:

$$\exp(-2ikD) = 1. \tag{4.9}$$

Using $1 = \exp(2\pi m)$, with $m \in \mathbb{Z}$, then above relation implies equality of the arguments of the exponentials:

$$2kD = 2\pi m \tag{4.10}$$

We rewrite the resonance condition by replacing in the above equation the relation between wavevector and wavelength, which is $k = 2\pi/\lambda$, and we obtain

$$2kD = 2\pi m \longrightarrow D = m\frac{\lambda}{2} \tag{4.11}$$

The resonance condition can also be expressed in terms of the laser's frequency, not wavelength. For an electromagnetic wave

$$\lambda = \frac{c}{\nu} \tag{4.12}$$

Therefore follows:

$$\nu_m = m\frac{c}{2D} \tag{4.13}$$

The resonance conditions derived, (4.11) and (4.13), tell us that, in order to bring an optical cavity into resonance, we can act on two parameters:

- 1. The length of the cavity, D, or,

- 2. the wavelength λ (or, equivalently, the frequency ν) of the laser.

Indeed, the condition (4.11) shows that resonance is achieved if the cavity length equals an integer multiple of half the laser wavelength. Changing the cavity length by $\Delta D = \lambda/2$, brings the cavity from one resonance (m) to the next one ($m+1$). Also, notice that if the cavity length increases

by $\lambda/2$, then the round trip length increases by λ, and the round trip phase increases by 2π. In other words, a cavity of length D and one of length $D + n\dfrac{\lambda}{2}$ behave identically for a given laser field.

Alternatively, expressing the condition in terms of frequency, shows that, for a fixed cavity length, resonance occurs only at discrete laser frequencies. These resonant frequencies are equally spaced, with a separation given by the Free Spectral Range (FSR):

$$\text{FSR} = \frac{c}{2D} \tag{4.14}$$

To summarise, we just learned what matters physically is the relative phase between the circulating field and the incoming laser field, and we can either:

- Act on the laser: if we change laser's frequency, we change the phase of the incoming field. By tuning the laser frequency appropriately, we can make the incoming field arrive in phase with the field already circulating in the cavity.

- Act on the cavity length: if we change D, we change the round trip phase accumulated by the field. By doing so, we determine an appropriate length such that the phase of the circulating field matches the phase of the laser field (which is fixed, unchanged).

4.1.3. How to scan over many resonances

Imagine we want to plot the circulating power inside an optical cavity as a function of some parameter, in order to clearly see how the cavity moves from resonance to anti-resonance and back again.

The question is, in a Fabry-Perot cavity used in interferometers, what is the typical variation of these parameters to enter on resonance? Let us consider parameters typical of the Advanced LIGO arm cavities:

- Arm length: D=4km, and,

- Laser wavelength: the default value in FINESSE is $\lambda = 1064$ nm, and corresponding laser frequency is $\dfrac{3 \times 10^8 \text{m/s}}{1064 \times 10^{-9}\text{m}} = 2.82 \times 10^{14}\text{Hz}$.

Adjacent resonances are separated by $\Delta D = \lambda/2 = 532$ nm: the mirror position must change by about half a micron, and this is a very small displacement compared to the 4 km cavity length. That's why in FINESSE distances are split in two parts, and we can write the following relation

$$D = D_0 + \delta D. \tag{4.15}$$

Here $D_0 = n\lambda$, so is the nearest integer multiple of the wavelength, such that D_0 is as close as possible to the true cavity length D. The remaining difference between D and L is the microscopic tuning. Instead of expressing this tiny length directly in meters, FINESSE expresses it as a phase:

$$\phi = 2\pi\frac{\delta D}{\lambda}. \tag{4.16}$$

In FINESSE, ϕ is given in degrees, so $360°$ corresponds to $\delta D = \lambda$, and $180°$ corresponds to $\delta D = \lambda/2$. Furthermore, this microscopic tuning is assigned to mirrors and beam splitters, not to free-space propagation. Practically, this means that, since the cavity is made by two mirrors,

changing its length by a small amount δD can be done: by moving mirror 1; by moving mirror 2; by moving both simultaneously. All these operations lead to the same physical effect, namely a change in the round-trip phase of the cavity.

For example, `m2.phi`, represents the microscopic tuning of mirror m2. So to conclude, the important takeaway is that a real cavity is a few kilometers long, but the resonant behaviour can be explored by changing a single phase parameter, which in turn corresponds to a nanometer change in the cavity length.

4.1.4. Fabry-Perot cavity properties

Another characteristic parameter of a cavity is its linewidth, usually given as its full width at half maximum (FWHM). In order to compute the linewidth we have to ask at which frequency the circulating power becomes half the maximum [1]:

$$\text{FWHM} = \frac{2\text{FSR}}{\pi} \arcsin \left(\frac{1 - r_1 r_2}{2\sqrt{r_1 r_2}} \right) \tag{4.17}$$

The ratio of the linewidth to the free spectral range is called the finesse of a cavity:

$$\mathcal{F} = \frac{\text{FSR}}{\text{FWHM}} = \frac{\pi}{2 \arcsin \left(\dfrac{1 - r_1 r_2}{2\sqrt{r_1 r_2}} \right)} \tag{4.18}$$

Cavities are often described in terms of $\mathcal{F}$ and FSR parameters, or equivalently $r_1 r_2$ and D. $\mathcal{F}$ provides photometric information about the mirrors, while FSR encodes geometrical information about the cavity. Both $\mathcal{F}$ and FWHM depend on $r_{1,2}$. As $r_{1,2}$ become higher, the finesse increases and FWHM decreases.

The storage time $\tau = \dfrac{1}{\pi \cdot \text{FWHM}}$ represents the average time spent by a photon inside the cavity, before escaping through one of the mirrors, and corresponds to a travel length of the photon of:

$$D_{\text{eq}} = \tau c = D \frac{2\mathcal{F}}{\pi} \tag{4.19}$$

It becomes evident that if the finesse increases, L_{eq} increases by the same amount. For instance, cavities used in the arms of aLIGO have a finesse $\mathcal{F} \approx 450$ [6], which corresponds to an equivalent arm length of $D_{eq} \approx 1150\,\text{km}$, rather than the actual physical length of $D = 4\,\text{km}$.

4.1.5. Fabry-Perot cavity as an effective mirror

So far, we have seen that lossless mirror is characterized by two numbers: a reflection coefficient r and a transmission coefficient t. Also, in this lossless case, energy conservation requires $|r|^2 + |t|^2 = 1$.

A Fabry–Perot cavity, even if made of two separate mirrors, can be treated, from the outside, as a single optical element with an effective reflection and transmission coefficients:

$$r_{cav} = a_4/a_0 = \frac{r_1 - r_2(t_1^2 + r_1^2)\exp(-2ikD)}{1 - r_1 r_2 \exp(-2ikD)} = \frac{r_1 - r_2 \exp(-2ikD)}{1 - r_1 r_2 \exp(-2ikD)} \tag{4.20}$$

$$t_{cav} = a_2/a_0 = -\frac{t_1 t_2 \exp(-ikD)}{1 - r_1 r_2 \exp(-2ikD)} \tag{4.21}$$

Let us simplify the notation by defining

$$-2kD = \delta \tag{4.22}$$

So:

$$r_{cav} = a_4/a_0 = \frac{r_1 - r_2\exp(i\delta)}{1 - r_1 r_2\exp(i\delta)} \tag{4.23}$$

And:

$$|r_{cav}|^2 = \frac{r_1^2 + r_2^2 - 2r_1 r_2 \cos\delta}{1 - 2r_1 r_2 \cos\delta + r_1^2 r_2^2} \tag{4.24}$$

Same calculations for t_{cav}:

$$t_{cav} = a_2/a_0 = -\frac{t_1 t_2\exp(i\delta/2)}{1 - r_1 r_2\exp(i\delta)} \tag{4.25}$$

and

$$|t_{cav}|^2 = \frac{t_1^2 t_2^2}{1 - 2r_1 r_2 \cos\delta + r_1^2 r_2^2} \tag{4.26}$$

Now we compute $|r_{cav}|^2 + t_{cav}|^2$ and we use $r_i^2 + t_i^2 = 1$, from which $t_i^2 = 1 - r_i^2$, and we prove that the identity always holds, independently of δ.

$$\begin{aligned}
|r_{cav}|^2 + |t_{cav}|^2 &= \frac{r_1^2 + r_2^2 - 2r_1 r_2 \cos\delta + (1 - r_1^2)(1 - r_2^2)}{1 - 2r_1 r_2 \cos\delta + r_1^2 r_2^2} \\
&= \frac{r_1^2 + r_2^2 - 2r_1 r_2 \cos\delta + 1 - r_1^2 - r_2^2 + r_1^2 r_2^2}{1 - 2r_1 r_2 \cos\delta + r_1^2 r_2^2} \\
&= \frac{1 - 2r_1 r_2 \cos\delta + r_1^2 r_2^2}{1 - 2r_1 r_2 \cos\delta + r_1^2 r_2^2} = 1
\end{aligned} \tag{4.27}$$

Let us now restrict ourselves to a simplified configuration consisting of a Fabry–Perot cavity and a mirror placed in front of it. This configuration is a simplification of the recycling cavities used in gravitational wave detectors: from the point of view of this additional mirror, the Fabry–Perot cavity behaves as an effective mirror whose reflection and transmission coefficients depend on the optical detuning. In the same way, the interferometer, viewed from the recycling port, can be treated as an effective optical element with a reflectivity frequency-dependent. Basically the role of the recycling cavities can be understood using the same concepts as a simple Fabry–Perot resonator.

4.2. Fundamental Principles in Optics

The primary theories for understanding light and optical phenomena are geometrical (or ray) and wave optics. Geometrical optics simplifies light into rays, while wave optics provides a more fundamental and comprehensive explanation, focusing on amplitude, phase, and wavefront information of light. Central to the theoretical underpinnings of the wave theory and study of light's properties are the Maxwell's equations. Maxwell's equations allow for the derivation of the wave equation.

$$\boxed{\nabla^2\Psi(r,t) = \frac{1}{c^2}\frac{\partial^2\Psi(r,t)}{\partial t^2}} \tag{4.28}$$

Equation 4.28 serves as the wave equation in vacuum. It uses a generalized notation to define any wave phenomena, including electromagnetic waves (light). Any wave phenomenon can be mathematically described by a real function of space $r = (x, y, z)$ and time t, typically represented as

$\Psi(r, t)$ and referred to as the wave function. Integral to this equation is speed at which the waveform or disturbance propagates through space and time. In vacuum this is equivalent to the speed of light, $\mathbf{c} = 2.9979 \times 10^8$ m/s. The wave equation is essentially a partial differential equation (PDE). This PDE can possess numerous solutions. We will represent the real wavefunction in complex notation in the form:

$$\Psi(r, t) = \psi(r)e^{-i2\pi\nu t}. \tag{4.29}$$

In this formulation, $\psi(r) = A(r)e^{i\varphi(r)}$ represents the time-independent or spatial component, commonly referred to as the complex amplitude of the wave function, ν denotes the temporal frequency of the wave, and the term $e^{-i2\pi\nu t}$ captures the time-varying aspect of the wave. The physical field is the real part of the complex field $\mathrm{Re}\{\Psi(r, t)\}$.

Usually our laser beams can be approximated to be paraxial. A wave is termed paraxial when its propagation direction is nearly parallel to a defined optical axis. More formally, a paraxial wave satisfies the condition that its angle of propagation (θ) with respect to the optical axis is small, that is, $\sin\theta \simeq \theta$. Laser beams are well-collimated and have small angular distribution, thus falling under the regime of the paraxial approximation. Now we have simplified the problem to find the solutions of the wave equation within the paraxial approximation/regime.

One of the solutions to the paraxial wave equation is the set of Hermite–Gauss (HG) modes. In this section, we elaborate on these modes and their analytical description. In particular, we focus on the fundamental Gaussian mode. It is important to understand the nature of these beams, as they are frequently discussed in the Finesse tutorials. A comprehensive and detailed treatment of these topics can be found in [1].

4.2.1. Gaussian mode

The most fundamental solution of the paraxial wave equation is the Gaussian mode. The mathematical description of Gaussian mode leads to a spatially confined and nondiverging beam - which represents the quality of laser beams. Lasers are the source of light and power in all GW detectors, through which we measure GWs. In this section we will define few characteristic parameters of the Gaussian beams.

The complex envelope $A(r)$ of Gaussian beam is given by,

$$A(r) = \frac{A_o}{q(z)} \exp\left[-ik\frac{x^2 + y^2}{2q(z)}\right], \quad q(z) = z + iz_R. \tag{4.30}$$

The quantity $q(z)$ is called the complex beam parameter of the beam and has to be imaginary to be able to satisfy the paraxial equation. It is defined using the real parameter z_R, which is known as the Rayleigh range. The q-parameter can be expressed in terms of its real and imaginary parts by defining two real functions - width w(z) and wavefront radius of curvature R(z) such that:

$$\frac{1}{q(z)} = \frac{1}{R(z)} - i\frac{\lambda}{\pi w^2(z)} \tag{4.31}$$

Substituting the q-parameter representation shown in equation 4.31 in equation 4.30, leads directly to the expression for the complex amplitude $\psi(r)$ of the Gaussian beam:
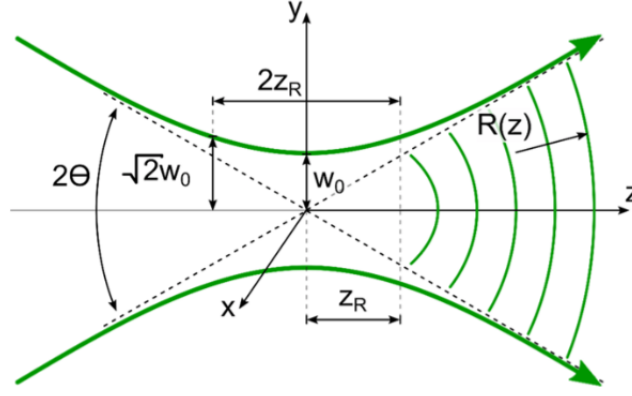
Figure 4.2: Evolution of the Gaussian beam size (radius) along the propagation axis [7].

$$\psi(r) = A_1 \frac{w_o}{w(z)} \exp\left[-\frac{x^2+y^2}{w^2(z)}\right] \exp\left[-ikz - ik\frac{x^2+y^2}{2R(z)} + i\tan^{-1}\left(\frac{z}{z_R}\right)\right] \tag{4.32}$$

$$w(z) = w_0\sqrt{1 + \left(\frac{z}{z_R}\right)^2} \tag{4.33}$$

$$R(z) = z\left[1 + \left(\frac{z_R}{z}\right)^2\right] \tag{4.34}$$

$$\xi(z) = \tan^{-1}\left(\frac{z}{z_R}\right). \tag{4.35}$$

In the Gaussian beam expression we have defined $A_1 = A_o/iz_R$. Each of these beam properties, as expressed in equations 4.33 to 4.35, will be further elaborated upon.

1. Beam radius: the beam width or radius, w(z), of a Gaussian beam is a parameter describing the transverse extent of the beam spot, and is defined as the radial distance from the beam's axis to where its intensity falls to $1/e^2$ (approximately 13.5%) of its peak intensity. The beam's narrowest point, known as the beam waist, is represented by w_o. The Rayleigh length, z_R, is defined by the condition that the beam width at z_R is $\sqrt{2}w_o$, indicating a doubling of the area of the beam's cross-section. The evolution of beam width for a Gaussian beam along the propagation axis (z) is shown in figure 4.2 and is described by the following mathematical relationship:

$$w(z) = w_o\sqrt{1 + \left(\frac{z}{z_R}\right)^2}.$$

2. RoC of the wavefronts: The other component of the complex beam parameters is R(z) - radius of curvature (RoC) of the laser beam wavefront.

$$R(z) = z\left[1 + \left(\frac{z_R}{z}\right)^2\right]. \tag{4.36}$$

At z=0, or at the waist of the beam, R(z) is infinite meaning that the wavefronts are planar. At $z = z_R$, the beam has the minimum radius i.e. maximum curvature. After the Rayleigh length the wavefronts of the beam are approximately similar as those of a spherical wave. The wavefronts of a Gaussian beam transition from being planar at z=0 to again becoming planar as z approaches infinity. Within this range, the beam transforms, adopting a spherical wavefront as it propagates through the z-domain.

3. Phase of the wavefronts: The phase term of the Gaussian beam as given by the equation 4.32 is,

$$\varphi(x, y, z) = kz + k\frac{x^2 + y^2}{2R(z)} - \tan^{-1}\left(\frac{z}{z_R}\right).$$

The first term, kz, represents the linear phase variation along the optical axis, similar to the phase accumulated by the wavefronts of a plane wave. The second term in the equation represents the quadratic phase variation in the transverse plane (x-y plane). As the beam propagates, the curvature of the wavefronts changes, leading to a corresponding change in the phase distribution across the beam profile. The third term is the Gouy phase. It is the extra longitudinal phase lag originating from the slower phase velocity of a Gaussian beam compared to a plane wave.

4.2.2. Higher Order Modes

The Gaussian mode represents the lowest-order solution to the paraxial approximation. It is distinguished by its single beam spot, symmetric intensity profile that diminishes in all directions away from the beam center. There are other solutions as well exhibiting more complex geometries and amplitude distributions in the transversal plane, correspondingly leading to a more obscure mathematical description. These solutions are often referred to as higher order modes (HOMs). In this section we will briefly introduce the Hermite-Gaussian (HG) mode.

4.2.3. Hermite-Gaussian Modes

Higher-order beam solutions can be found by solving the paraxial wave equation. One family of the resulting solutions is named as HG_{lm}. The HG mode is distinguished by their unique spatial distributions, which can exhibit multiple peaks along both the horizontal and vertical axes. Such modes exhibit non-Gaussian amplitude distributions but share the wavefronts (RoC) of the Gaussian beam. The complex field amplitude for HG modes can be defined by:

$$\psi_{l,m}(r) = A_{l,m}\left[\frac{w_0}{w(z)}\right]G_l\left(\frac{\sqrt{2}x}{w(z)}\right)G_m\left(\frac{\sqrt{2}y}{w(z)}\right) \times \exp\left[-ikz - ik\frac{x^2 + y^2}{2R(z)} + i(l + m + 1)\zeta(z)\right]$$

(4.37)

where

$$G_l(u) = H_l(u)e^{(-u^2/2)}$$

is known as the HG-function. H_l and H_m are Hermite polynomials. The first few Hermite polynomials equal

$$H_0(x) = 1, \quad H_1(x) = 2x, \quad H_2(x) = 4x^2 - 2 \quad \text{and} \quad H_3(x) = 8x^3 - 12. \tag{4.38}$$
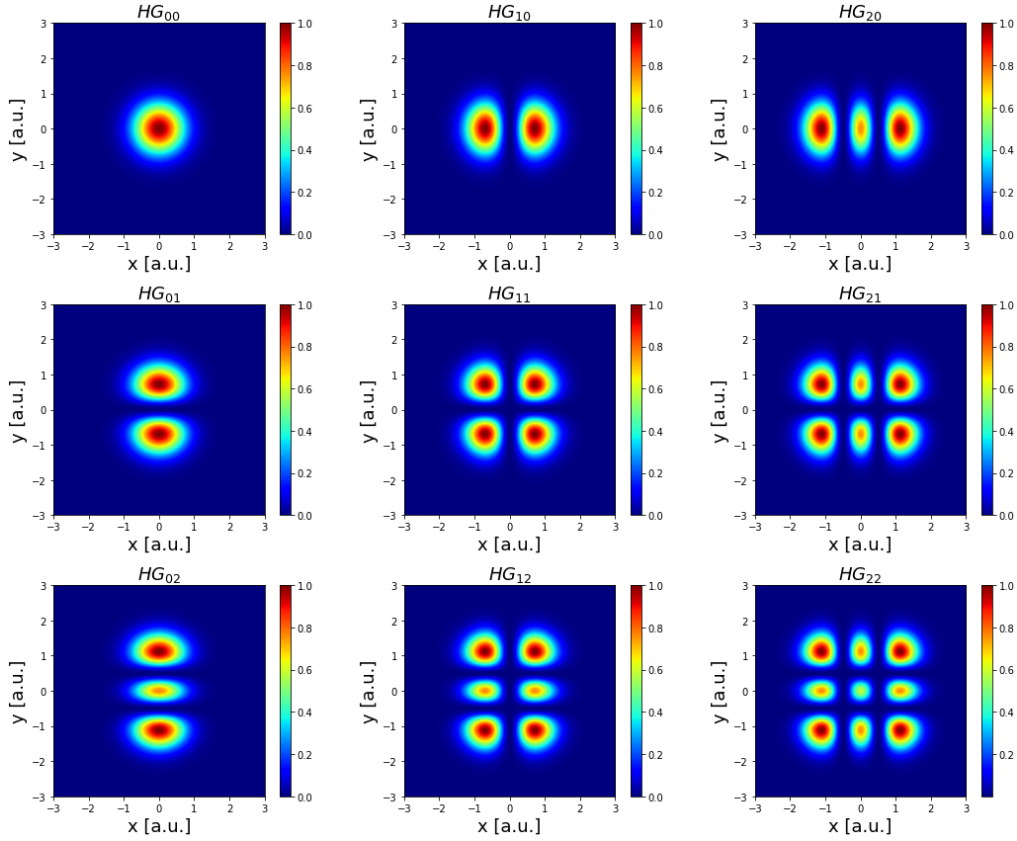
Figure 4.3: Intensity distribution of first few Hermite-Gaussian beams. The HG_{00} represents the fundamental Gaussian beam.

Figure 4.3 represents intensity distribution of few lower order HG modes. The HG_{00} mode where the Hermite polynomials is equal to 1, is the fundamental TEM_{00} or Gaussian mode. Similar to HG modes, the paraxial wave equation allows other higher-order solutions, with Laguerre-Gaussian modes being among the significant ones. The key takeaway is that in complex optical systems featuring multiple resonating cavities, HOMs may resonate within the system.
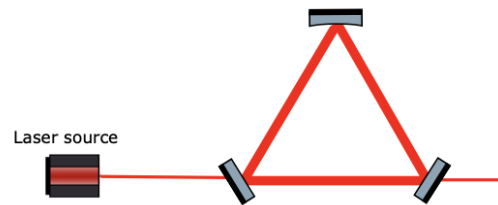
5. Goal of this workshop

In the gravitational wave community, modeling plays an essential role in the detector design and operation. Such detectors are extremely complex, in the sense that their operation depends on a large number of parameters. In this workshop, you will be introduced to modeling with FINESSE, a frequency-domain simulation tool, with an emphasis on studying the different cavity geometries and the effects of imperfections in these optical cavities.
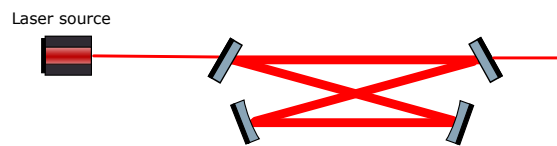
The three different cavity configurations under study are presented below:

(a) Fabry-Perot cavity

(b) Triangular cavity

3

(c) Bow tie cavity

Figure 5.1: Cavity geometries under study.

References

[1] C. Bond, D. Brown, A. Freise, and K.A. Strain. Interferometer techniques for gravitational-wave detection. *Living Reviews in Relativity*, 19(3), 2016.

[2] The LIGO Collaboration. Advanced LIGO. *Classical and Quantum Gravity*, 32(7):074001, 2015.

[3] The Virgo Collaboration. Advanced Virgo: A second-generation interferometric gravitational wave detector. *Classical and Quantum Gravity*, 32(2):024001, 2015.

[4] KAGRA Collaboration. Overview of KAGRA: Detector design and construction history. *Progress of Theoretical and Experimental Physics*, 2020(5), 2020.

[5] K. Dooley, J. Leong, T. Adams, C. Affeldt, A. Bisht, C. Bogan, J. Degallaix, C. Gräf, S. Hild, J. Hough, and et al. GEO 600 and the GEO-HF upgrade program: Successes and challenges. *Classical and Quantum Gravity*, 33, 2015.

[6] J. Aasi et al. (The LIGO Scientific Collaboration). Advanced LIGO. *Classical and Quantum Gravity*, 32:074001, 2015.

[7] Michael Kovalev, Iliya Gritsenko, Nikita Stsepuro, Pavel Nosov, George Krasin, and Sergey Kudryashov. Reconstructing the spatial parameters of a laser beam using the transport-of-intensity equation. *Sensors*, 22(5):1765, 2022.